

# Multiplicity dependence of identical particle correlations in the quantum optical approach

N. Suzuki

*Matsusho Gakuen Junior College, Matsumoto 390-1295, Japan*

M. Biyajima

*Department of Physics, Shinshu University, Matsumoto 390-8621, Japan*

(Received 8 February 1999; published 10 August 1999)

Identical particle correlations at fixed multiplicity are considered in the presence of chaotic and coherent fields. The multiplicity distribution, one-particle momentum density, and two-particle correlation function are obtained based on the diagrammatic representation for cumulants in semi-inclusive events. Our formulation is applied to the analysis of the experimental data on the multiplicity dependence of correlation functions reported by the UA1 and the OPAL Collaborations. [S0556-2813(99)07008-9]

PACS number(s): 25.75.Gz, 05.30.Jp

## I. INTRODUCTION

In high energy hadron-hadron collisions, Bose-Einstein correlations of the identical particles are considered as one of the possible measures for the space-time domain where identical particles are produced. One of the theoretical approaches to the Bose-Einstein correlations is made on the analogy of the quantum optics [1], where two types of sources, chaotic and coherent, are introduced. A diagrammatical method, based on the Glauber-Lachs formula [1], has been proposed [2] to find the higher order Bose-Einstein correlation (BEC) functions in the quantum optical (QO) approach. In Ref. [3], the generating functional (GF) for momentum densities is derived in the QO approach, and a diagrammatic representation for cumulants is proposed.

Up to the present, identical particle correlations in fixed multiplicity events have been investigated in the case of purely chaotic fields. Two-particle correlations are analyzed in Ref. [4] by using Monte Carlo methods. The multiplicity dependence of one-particle distributions is discussed in Ref. [5], and that of two- or three-particle correlations is considered in Ref. [6].

In Ref. [7], an outline of our formulation on particle correlations at fixed multiplicity in the QO approach has been briefly reported. General features of multiplicity distributions, one-particle distributions, and two-particle correlations at fixed multiplicity have been also shown. In the present paper, identical particle correlations at fixed multiplicity in the QO approach are considered in detail. The diagrammatic representation for cumulants is used to obtain the formulas in semi-inclusive events in an analogous way to that in inclusive events [3]. Furthermore, our formulas are applied to analyses of the experimental data in  $p\bar{p}$  collisions by the UA1 Collaboration [8] and in  $e^+e^-$  collisions by the OPAL Collaboration [9].

At first, we consider the case when there are no correlations among produced particles in the final states. Then particles in the final states are given by a coherent state,

$$|\phi\rangle = \exp\left[-\frac{1}{2}\int |f(p)|^2 \frac{d^3p}{E} + \int f(p) a^\dagger(p) \frac{d^3p}{E}\right] |0\rangle. \quad (1)$$

The  $n$ -particle momentum density in semi-inclusive events is defined by

$$\begin{aligned} \rho_n(p_1, \dots, p_n) &= \frac{1}{\sigma_{\text{inel}}} E_1 \cdots E_n \frac{d^{3n} \sigma_{\text{inel}}}{d^3 p_1 \cdots d^3 p_n} \\ &= |\langle 0 | a(p_1) \cdots a(p_n) | \phi \rangle|^2, \end{aligned}$$

which is reduced to

$$\rho_n(p_1, \dots, p_n) = |f(p_1)|^2 \cdots |f(p_n)|^2 \exp\left[-\int |f(p)|^2 \frac{d^3p}{E}\right]. \quad (2)$$

In the QO approach, the function  $f(p)$  is divided into two parts:

$$f(p) = \sum_{i=1}^M a_i \phi_i(p) + f_c(p), \quad (3)$$

where  $\phi_i(p)$  and  $f_c(p)$  are amplitudes of the  $i$ th chaotic source and a coherent source, and  $a_i$  is a random complex number attached to the  $i$ th chaotic source. In addition,  $M$  is the number of independent chaotic sources [3], which is regarded to be infinite in the present paper. The  $n$ -particle momentum density in the QO approach [10] is defined by

$$\begin{aligned} \rho_n(p_1, \dots, p_n) &= \left\langle |f(p_1)|^2 \cdots |f(p_n)|^2 \right. \\ &\quad \left. \times \exp\left[-\int |f(p)|^2 \frac{d^3p}{E}\right] \right\rangle_a. \quad (4) \end{aligned}$$

In Eq. (4), the angular brackets  $\langle F \rangle_a$  denote an average of  $F$  over the random number  $a_i$  with a Gaussian weight [1]:

$$\langle F \rangle_a = \prod_{i=1}^M \left( \frac{1}{\pi \lambda_i} \int \exp\left[-\frac{|a_i|^2}{\lambda_i}\right] d^2 a_i \right) F. \quad (5)$$

It should be noticed that the classical (pion) fields are randomized in our approach. On the other hand, each mode

of light is randomized in the quantum optics [1]. After the average is taken over the random number  $a_i$  in Eq. (5), terms composed of  $a_i^l a_i^{*m}$  in the function  $F$  vanish if  $l \neq m$ .

The generating functional for momentum densities in semi-inclusive events is defined by the following equation:

$$Z_{\text{sm}}[h(p)] = \sum_{n=1}^{\infty} \frac{1}{n!} \int \cdots \int \rho_n(p_1, \dots, p_n) \times h(p_1) \dots h(p_n) \frac{d^3 p_1}{E_1} \cdots \frac{d^3 p_n}{E_n}. \quad (6)$$

From Eqs. (4) and (6), the GF is written formally as

$$Z_{\text{sm}}[h(p)] = \left\langle \exp \left[ \int |f(p)|^2 [h(p) - 1] \frac{d^3 p}{E} \right] \right\rangle_a. \quad (7)$$

On the right hand side of Eq. (6), an additional constant  $Z_{\text{sm}}[h(p)=0]$ , which does not affect to the momentum densities, is added. Inversely, the  $n$ -particle momentum density in the semi-inclusive events is given from the GF as

$$\rho_n(p_1, \dots, p_n) = E_1 \cdots E_n \frac{\delta^n Z_{\text{sm}}[h(p)]}{\delta h(p_1) \cdots \delta h(p_n)} \Big|_{h(p)=0}.$$

From the sum rule between semi-inclusive and inclusive cross sections [11], the GF  $Z[h(p)]$  for inclusive events is connected to that for semi-inclusive events:

$$Z[h(p)] = Z_{\text{sm}}[h(p) + 1] = \left\langle \exp \left[ \int |f(p)|^2 h(p) \frac{d^3 p}{E} \right] \right\rangle_a. \quad (8)$$

The  $n$ -particle inclusive momentum density is given by

$$\rho_{\text{in}}(p_1, \dots, p_n) = E_1 \cdots E_n \frac{\delta^n Z[h(p)]}{\delta h(p_1) \cdots \delta h(p_n)} \Big|_{h(p)=0}.$$

The explicit form of the GF, Eq. (8), is shown in Ref. [3], and the higher order BEC functions in inclusive events are obtained from it. In the following section, we would like to show that we can obtain higher order momentum densities in semi-inclusive events by analogy with a derivation in inclusive events.

## II. GENERATING FUNCTIONAL AND CUMULANT

In the following, we slightly change the definition of the GF from Eq. (7) to

$$Z_{\text{sm}}[h(p)] = c_0 \left\langle \exp \left[ \int |f(p)|^2 h(p) \frac{d^3 p}{E} \right] \right\rangle_a, \quad (9)$$

where the exponential damping factor in Eq. (7) is replaced by a normalization constant  $c_0$ . Then, the  $n$ -particle momentum density in the QO approach is given by

$$\begin{aligned} \rho_n(p_1, \dots, p_n) &= E_1 \cdots E_n \frac{\delta^n Z[h(p)]}{\delta h(p_1) \cdots \delta h(p_n)} \Big|_{h(p)=0} \\ &= c_0 \langle |f(p_1) \cdots f(p_n)|^2 \rangle_a. \end{aligned} \quad (10)$$

The GF  $G_{\text{sm}}[h(p)]$  for cumulants is defined by the equation

$$G_{\text{sm}}[h(p)] \equiv \ln Z_{\text{sm}}[h(p)], \quad (11)$$

and the  $n$ th order cumulant is given by

$$g_n(p_1, \dots, p_n) = E_1 \cdots E_n \frac{\delta^n G_{\text{sm}}[h(p)]}{\delta h(p_1) \cdots \delta h(p_n)} \Big|_{h(p)=0}. \quad (12)$$

From Eqs. (10), (11), and (12), we have iteration relations for momentum densities,

$$\rho_1(p_1) = c_0 g_1(p_1),$$

$$\begin{aligned} \rho_n(p_1, \dots, p_n) &= g_1(p_1) \rho_{n-1}(p_2, \dots, p_n) \\ &\quad + \sum_{i=1}^{n-2} \sum g_{i+1}(p_1, p_{j_1}, \dots, p_{j_i}) \\ &\quad \times \rho_{n-i-1}(p_{j_{i+1}}, \dots, p_{j_{n-1}}) \\ &\quad + c_0 g_n(p_1, \dots, p_n). \end{aligned} \quad (13)$$

The second summation on the right hand side of Eq. (13) indicates that all possible combinations of  $(j_1, \dots, j_i)$  and  $(j_{i+1}, \dots, j_{n-1})$  are taken from  $(2, 3, \dots, n)$ . Equation (13) shows that the  $n$ -particle momentum density  $\rho_n(p_1, \dots, p_n)$  ( $n=1, 2, \dots$ ) can be evaluated if the cumulant  $g_n(p_1, \dots, p_n)$  ( $i=1, 2, \dots, n$ ) is obtained.

The semi-inclusive one-particle and two-particle cumulants are given from Eq. (12), respectively, as

$$g_1(p_1) = \langle f(p_1) \rangle_a = r(p_1, p_1) + c(p_1, p_1),$$

$$g_2(p_1, p_2) = \langle f(p_1) f(p_2) \rangle_a - \langle f(p_1) \rangle_a \langle f(p_2) \rangle_a$$

$$= |r(p_1, p_2)|^2 + 2\text{Re}[r(p_1, p_2)c(p_2, p_1)],$$

where  $r(p_1, p_2)$  is a correlation caused by the chaotic sources and  $c(p_1, p_2)$  is a correlation by the coherent source. Those are given by

$$\begin{aligned} r(p_1, p_2) &= \sum_{i=1}^M \lambda_i \phi_i(p_1) \phi_i^*(p_2), \\ c(p_1, p_2) &= f_c(p_1) f_c^*(p_2). \end{aligned} \quad (14)$$

As the GF, Eq. (9), in semi-inclusive events is the same with the GF, Eq. (8), in inclusive events except for the normalization factor  $c_0$ , the cumulants of semi-inclusive events are also calculated from the same diagrammatic presentation

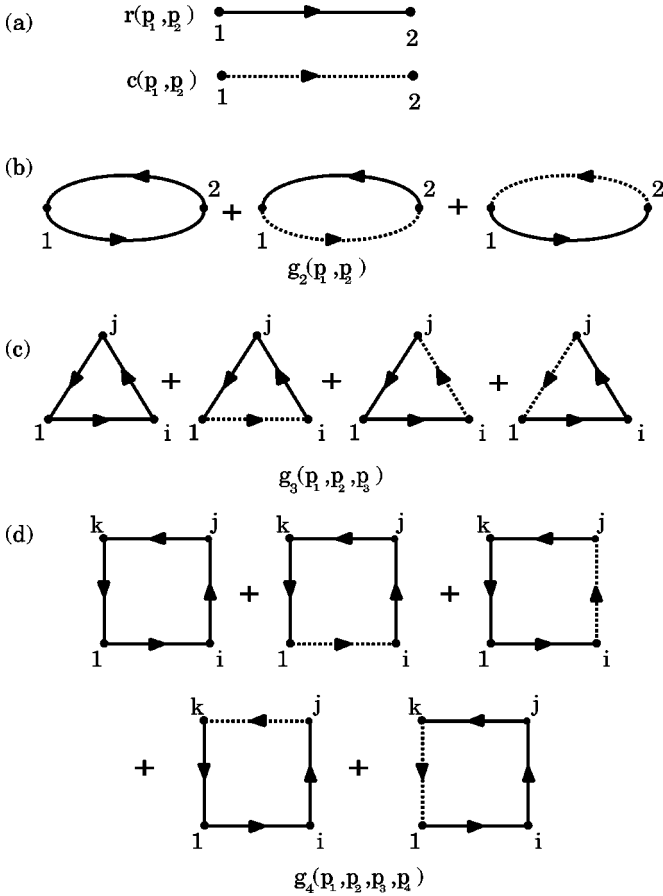


FIG. 1. Diagrammatic representation for cumulants in semi-inclusive events. (a) Contribution from the chaotic field,  $r(p_1, p_2)$ , is shown by the solid line with arrow orienting from point 1 to 2. That of the coherent field,  $c(p_1, p_2)$ , is shown by dotted line with arrow from 1 to 2. (b) Diagram for  $g_2(p_1, p_2)$ . (c) Diagram for  $g_3(p_1, p_2, p_3)$ . All permutations of (2,3) should be taken for (i,j). (d) Diagram for  $g_4(p_1, \dots, p_4)$ . Those of (2,3,4) should be taken for (i,j,k).

as those of inclusive events [3]. A diagrammatic representation for them up to fourth order is shown in Fig. 1.

The  $n$ th order cumulant is made up of connected terms of the correlations  $r_{ij}$  of chaotic fields and those  $c_{ij}$  of the coherent field. If  $n \geq 3$ , the  $n$ th order cumulant  $g_n(p_1, \dots, p_n)$  is simply expressed by using the  $n$ -gon. The  $n$ th order cumulant consists of two types of terms: one is made only of the correlations of the chaotic fields, and the other contains the correlations both of the chaotic fields and of the coherent field. One of the terms belonging to the former type is given by  $r_{12}r_{23} \cdots r_{(n-1)n}r_{n1}$ . It can be expressed by the circular permutation (12...n) started from 1. Other terms can be made from (12...n) by any permutation. Therefore, there are  $(n-1)!$  different terms in the former type. If any one of the correlations  $r_{ij}$  of the chaotic fields, belonging to the former type, is replaced by the correlation  $c_{ij}$  of the coherent field, terms of the latter type are made. Therefore, there are  $n!$  different terms in the latter type. It should be noted that half of the terms in the  $n$ th order cumulant are complex conjugates to the other half.

### III. BASIC FORMULAS AT FIXED MULTIPLICITY

In order to calculate momentum densities at fixed multiplicity, the  $k$ -particle momentum density and  $k$ th order cumulant at  $n$ -particle events ( $k \leq n$ ) are defined by the following equations, respectively:

$$\rho_n^{(k)}(p_1, \dots, p_k) = \frac{1}{(n-k)!} \int \cdots \int \rho_n(p_1, \dots, p_k, p_{k+1}, \dots, p_n) \times \frac{d^3 p_{k+1}}{E_{k+1}} \cdots \frac{d^3 p_n}{E_n},$$

$$g_n^{(k)}(p_1, \dots, p_k) = \frac{1}{(n-k)!} \int \cdots \int g_n(p_1, \dots, p_k, p_{k+1}, \dots, p_n) \times \frac{d^3 p_{k+1}}{E_{k+1}} \cdots \frac{d^3 p_n}{E_n}. \quad (15)$$

The GF for multiplicity distribution  $P(n)$  is given from Eq. (9) if the function  $h(p)$  is independent of momentum  $p$ :

$$Z_{\text{sm}}(h) = c_0 \left\langle \exp \left[ \int |f(p)|^2 \frac{d^3 p}{E} h \right] \right\rangle_a. \quad (16)$$

The multiplicity distribution is given from Eq. (16):

$$P(n) = \frac{1}{n!} \left. \frac{\partial^n Z_{\text{sm}}(h)}{\partial h^n} \right|_{h=0} = \frac{1}{n!} \rho_n^{(0)}. \quad (17)$$

The normalization of the  $k$ -particle momentum density at  $n$ -particle events is given by

$$\int \cdots \int \rho_n^{(k)}(p_1, \dots, p_k) \frac{d^3 p_1}{E_1} \cdots \frac{d^3 p_k}{E_k} = \frac{n!}{(n-k)!} P(n).$$

Then the normalized  $k$ -particle momentum density in  $n$ -particle events is defined as

$$\tilde{\rho}_n^{(k)}(p_1, \dots, p_k) = \frac{(n-k)!}{n!} \frac{\rho_n^{(k)}(p_1, \dots, p_k)}{P(n)}. \quad (18)$$

In general, the inclusive  $k$ -particle momentum density is given from the semi-inclusive momentum densities as

$$\rho_{\text{in}}^{(k)}(p_1, \dots, p_k) = \sum_{n=k} \rho_n^{(k)}(p_1, \dots, p_k),$$

which satisfies

$$\int \cdots \int \rho_{\text{in}}^{(k)}(p_1, \dots, p_k) \frac{d^3 p_1}{E_1} \cdots \frac{d^3 p_k}{E_k} = \sum_{n=k} \frac{n!}{(n-k)!} P(n).$$

It should be noted that if the  $k$ th order inclusive momentum density is integrated over all of the momenta, it becomes the  $k$ th order factorial moment.

From Eqs. (13), (15), and (17), the multiplicity distribution and particle densities in semi-inclusive events up to third order can be expressed by the following recurrence equations:

$$P(n) = \frac{1}{n} \sum_{j=1}^n j g_j^{(0)} P(n-j), \quad (19)$$

$$\rho_n^{(1)}(p_1) = \sum_{j=1}^n g_j^{(1)}(p_1) P(n-j), \quad (20)$$

$$\begin{aligned} \rho_n^{(2)}(p_1, p_2) &= \sum_{j=1}^{n-1} g_j^{(1)}(p_1) \rho_{n-j}^{(1)}(p_2) \\ &+ \sum_{j=2}^n g_j^{(2)}(p_1, p_2) P(n-j), \end{aligned} \quad (21)$$

$$\begin{aligned} \rho_n^{(3)}(p_1, p_2, p_3) &= \sum_{j=1}^{n-2} g_j^{(1)}(p_1) \rho_{n-j}^{(2)}(p_2, p_3) \\ &+ \sum_{j=2}^{n-1} \{g_j^{(2)}(p_1, p_2) \rho_{n-j}^{(1)}(p_3) \\ &+ g_j^{(2)}(p_1, p_3) \rho_{n-j}^{(1)}(p_2)\} \\ &+ \sum_{j=3}^n g_j^{(3)}(p_1, p_2, p_3) P(n-j), \end{aligned} \quad (22)$$

where  $P(0) = c_0$ . On the other hand, cumulants at fixed multiplicity are obtained from Fig. 1 as

$$g_1^{(0)} = \Delta_1^{(R)} + \Delta_0^{(S)},$$

$$g_n^{(0)} = \frac{1}{n} \left[ \Delta_n^{(R)} + 2\Delta_{n-1}^{(S)} + \sum_{j=1}^{n-2} \Delta_{j, n-j-1}^{(T)} \right], \quad n = 2, 3, \dots, \quad (23)$$

$$g_1^{(1)}(p_1) = r(p_1, p_1) + c(p_1, p_1),$$

$$g_n^{(1)}(p_1) = R_n(p_1, p_1) + 2S_{n-1}(p_1, p_1) + \sum_{j=1}^{n-2} T_{j, n-j-1}(p_1, p_1), \quad n = 2, 3, \dots, \quad (24)$$

$$\begin{aligned} g_n^{(2)}(p_1, p_2) &= \sum_{j=1}^{n-1} R_j(p_1, p_2) R_{n-j}(p_2, p_1) + 2c(p_1, p_2) R_{n-1}(p_2, p_1) + 2 \sum_{j=1}^{n-2} \{S_j(p_1, p_2) R_{n-j-1}(p_2, p_1) \\ &+ R_{n-j-1}(p_1, p_2) S_j(p_2, p_1)\} + \sum_{j=1}^{n-3} \sum_{l=1}^{n-j-2} \{T_{j,l}(p_1, p_2) R_{n-j-l-1}(p_2, p_1) + R_{n-j-l-1}(p_1, p_2) T_{j,l}(p_2, p_1)\}, \end{aligned} \quad (25)$$

$$\begin{aligned} g_n^{(3)}(p_1, p_2, p_3) &= \sum_{j=1}^{n-2} \sum_{l=1}^{n-j-1} \{R_j(p_1, p_2) R_l(p_2, p_3) R_{n-j-l}(p_3, p_1) + R_j(p_1, p_3) R_l(p_3, p_2) R_{n-j-l}(p_2, p_1)\} \\ &+ 2 \sum_{j=1}^{n-2} \{c(p_1, p_2) R_j(p_2, p_3) R_{n-j-1}(p_3, p_1) + c(p_1, p_3) R_j(p_3, p_2) R_{n-j-1}(p_2, p_1) \\ &+ c(p_2, p_3) R_{n-j-1}(p_3, p_1) R_j(p_1, p_2)\} + \sum_{j=1}^{n-3} \sum_{l=1}^{n-j-2} \{S_j(p_1, p_2) R_l(p_2, p_3) R_{n-j-l-1}(p_3, p_1) \\ &+ S_j(p_1, p_3) R_l(p_3, p_2) R_{n-j-l-1}(p_2, p_1) + R_j(p_1, p_2) S_l(p_2, p_3) R_{n-j-l-1}(p_3, p_1) \\ &+ R_j(p_1, p_3) S_l(p_3, p_2) R_{n-j-l-1}(p_2, p_1) + R_j(p_1, p_2) R_{n-j-l-1}(p_2, p_3) S_l(p_3, p_1) \\ &+ R_j(p_1, p_3) R_{n-j-l-1}(p_3, p_2) S_l(p_2, p_1)\} \\ &+ \sum_{j=1}^{n-4} \sum_{l=1}^{n-j-3} \sum_{m=1}^{n-j-l-2} \{T_{j,l}(p_1, p_2) R_m(p_2, p_3) R_{n-j-l-m-1}(p_3, p_1) \\ &+ T_{j,l}(p_1, p_3) R_m(p_3, p_2) R_{n-j-l-m-1}(p_2, p_1) + R_m(p_1, p_2) T_{j,l}(p_2, p_3) R_{n-j-l-m-1}(p_3, p_1) \\ &+ R_m(p_1, p_3) T_{j,l}(p_3, p_2) R_{n-j-l-m-1}(p_2, p_1) + R_m(p_1, p_2) R_{n-j-l-m-1}(p_2, p_3) T_{j,l}(p_3, p_1) \\ &+ R_m(p_1, p_3) R_{n-j-l-m-1}(p_3, p_2) T_{j,l}(p_2, p_1)\}, \end{aligned} \quad (26)$$

where

$$\begin{aligned}
 R_1(p_1, p_2) &= r(p_1, p_2), \\
 R_n(p_1, p_2) &= \int r(p_1, k) R_{n-1}(k, p_2) \frac{d^3 k}{\omega}, \quad n=2, 3, \dots, \\
 S_0(p_1, p_2) &= c(p_1, p_2), \\
 S_n(p_1, p_2) &= \int c(p_1, k) R_n(k, p_2) \frac{d^3 k}{\omega}, \quad n=1, 2, \dots, \\
 T_{j,l}(p_1, p_2) &= \int \int R_j(p_1, k_1) c(k_1, k_2) R_l(k_2, p_2) \frac{d^3 k_1}{\omega_1} \frac{d^3 k_2}{\omega_2}, \quad (27) \\
 \Delta_n^{(R)} &= \int R_n(k, k) \frac{d^3 k}{\omega}, \\
 \Delta_n^{(S)} &= \int S_n(k, k) \frac{d^3 k}{\omega},
 \end{aligned}$$

$$\Delta_{j,l}^{(T)} = \int T_{j,l}(k, k) \frac{d^3 k}{\omega}. \quad (28)$$

In the following, variables are changed from  $(p_{1L}, \mathbf{p}_{1T})$  to  $(y_1, \mathbf{p}_{1T})$ , with rapidity  $y_1 = \tanh^{-1}(p_{1L}/E_1)$ . Both correlations  $r(p_1, p_2)$  and  $c(p_1, p_2)$  are assumed to be real and parametrized as

$$\begin{aligned}
 r(y_1, \mathbf{p}_{1T}; y_2, \mathbf{p}_{2T}) &= p \sqrt{\rho(y_1, \mathbf{p}_{1T}) \rho(y_2, \mathbf{p}_{2T})} I(\Delta y, \Delta \mathbf{p}_T), \\
 c(y_1, \mathbf{p}_{1T}; y_2, \mathbf{p}_{2T}) &= (1-p) \sqrt{\rho(y_1, \mathbf{p}_{1T}) \rho(y_2, \mathbf{p}_{2T})}, \\
 \rho(y_1, \mathbf{p}_{1T}) &= \langle n_0 \rangle \sqrt{\frac{\pi}{\alpha} \frac{\pi}{\beta}} \exp[-\alpha y_1^2 - \beta \mathbf{p}_{1T}^2], \\
 I(\Delta y, \Delta \mathbf{p}_T) &= \exp[-\gamma_L (\Delta y)^2 - \gamma_T (\Delta \mathbf{p}_T)^2], \quad (29)
 \end{aligned}$$

where  $p = r(p_i, p_i)/\rho(p_i)$  is called the chaoticity parameter,  $\Delta y = y_2 - y_1$ , and  $\Delta \mathbf{p}_T = \mathbf{p}_{2T} - \mathbf{p}_{1T}$ . Functions defined by Eqs. (27), (28), and (29) are expressed as

$$\begin{aligned}
 R_j(y_1, \mathbf{p}_{1T}, y_2, \mathbf{p}_{2T}) &= N_j \exp[-A_j (y_1^2 + y_2^2) + 2C_j y_1 y_2] \exp[-U_j (\mathbf{p}_{1T}^2 + \mathbf{p}_{2T}^2) + 2W_j \mathbf{p}_{1T} \cdot \mathbf{p}_{2T}], \\
 S_j(y_1, \mathbf{p}_{1T}, y_2, \mathbf{p}_{2T}) &= \frac{(1-p) \langle n_0 \rangle \alpha^{1/2} \beta}{\sqrt{A_j + \alpha/2} (U_j + \beta/2)} N_j \exp\left[-\frac{\alpha}{2} y_1^2 - \left(\frac{\alpha}{2} + \frac{\alpha \gamma_L}{A_j + \alpha/2}\right) y_2^2\right] \exp\left[-\frac{\beta}{2} \mathbf{p}_{1T}^2 - \left(\frac{\beta}{2} + \frac{\beta \gamma_T}{A_j + \beta/2}\right) \mathbf{p}_{2T}^2\right], \\
 T_{i,j}(y_1, \mathbf{p}_{1T}, y_2, \mathbf{p}_{2T}) &= \frac{(1-p) \langle n_0 \rangle \pi^{3/2} \alpha^{1/2} \beta}{\sqrt{(A_i + \alpha/2)(A_j + \alpha/2)(U_i + \beta/2)(U_j + \beta/2)}} N_i N_j \\
 &\quad \times \exp\left[-\left(\frac{\alpha}{2} + \frac{\alpha \gamma_L}{A_i + \alpha/2}\right) y_1^2 - \left(\frac{\alpha}{2} + \frac{\alpha \gamma_L}{A_j + \alpha/2}\right) y_2^2\right] \exp\left[-\left(\frac{\beta}{2} + \frac{\beta \gamma_T}{A_i + \beta/2}\right) \mathbf{p}_{1T}^2 - \left(\frac{\beta}{2} + \frac{\beta \gamma_T}{A_j + \beta/2}\right) \mathbf{p}_{2T}^2\right], \quad (30)
 \end{aligned}$$

where

$$\begin{aligned}
 A_1 &= \frac{\alpha}{2} + \gamma_L, \quad C_1 = \gamma_L, \\
 A_{j+1} &= A_1 - \frac{\gamma_L^2}{A_j + A_1}, \quad C_{j+1} = \frac{\gamma_L C_j}{A_j + A_1}, \\
 U_1 &= \frac{\beta}{2} + \gamma_T, \quad W_1 = \gamma_T, \\
 U_{j+1} &= U_1 - \frac{\gamma_T^2}{U_j + U_1}, \quad W_{j+1} = \frac{\gamma_T W_j}{U_j + U_1}, \\
 N_1 &= p \langle n_0 \rangle \frac{\alpha^{1/2} \beta}{\pi^{3/2}},
 \end{aligned}$$

$$N_{j+1} = \frac{p \langle n_0 \rangle \alpha^{1/2} \beta}{\sqrt{A_j + A_1} (U_j + U_1)} N_j. \quad (31)$$

#### IV. ANALYSES OF EXPERIMENTAL DATA

Our formulas are applied to analyses of negatively charged particles, or like-sign particles. Recently, preliminary data of identical two-particle correlations in semi-inclusive events in  $p\bar{p}$  collisions at  $\sqrt{s} = 900$  GeV within the pseudorapidity interval from  $-3.0$  to  $3.0$  have been reported by the UA1 Collaboration [8]. As can be seen from Eq. (21), the multiplicity distribution and one-particle densities are included in the formula of the two-particle density; at least the multiplicity distribution of the same data sample is required to analyze the two-particle correlation. The multiplicity distribution at  $\sqrt{s} = 900$  GeV is also reported by the UA1 group [12]. However, the data are taken within the pseudorapidity interval from  $-2.5$  to  $2.5$ . In the present analysis, those data

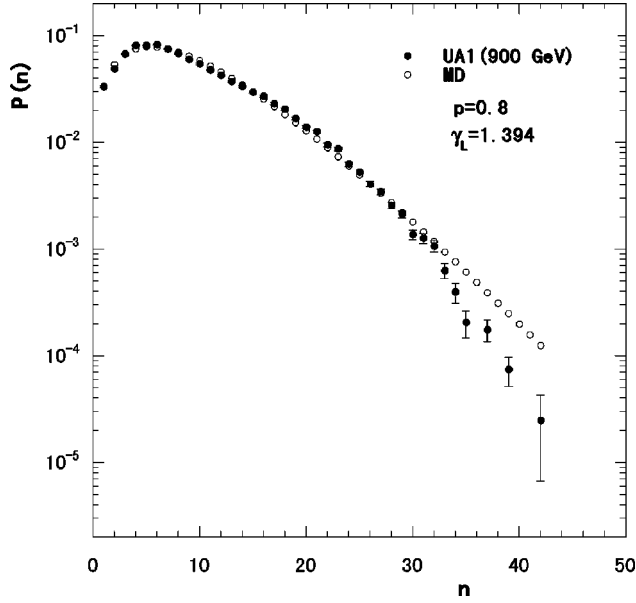


FIG. 2. Multiplicity distribution observed in  $p\bar{p}$  collisions [14] is analyzed by our formula. Parameters are determined by the minimum chi-squared method:  $p=0.8$ ,  $\langle n_0 \rangle=2.584$ , and  $\gamma_L=1.394$ .

are used to adjust the parameters included in our formulation.

The parameter  $\alpha$  is determined from the parametrization of one-particle rapidity distribution of Landau's hydrodynamical model [13], and  $\beta$  is taken from the inclusive transverse momentum distribution. In the present analysis, we neglect the correlation in transverse momentum space; in other words,  $\gamma_T$  is taken to be zero, and the calculated value is compared with the data after being integrated over the transverse momentum. Therefore, the parametrization of  $\beta$  does not affect the calculated results. Those values are taken as

$$\alpha=0.25, \quad \beta=5.556, \quad \gamma_T=0.$$

The multiplicity distribution is normalized to satisfy

$$\sum_{n=1}^{n_{\max}} P(n)=1, \quad (32)$$

where  $n_{\max}=42$  is the maximum multiplicity of the observed negatively charged particles.

Other parameters are adjusted to fit the multiplicity distribution [12] from  $n=1$  to  $n=35$  in the following way. The chaoticity parameter  $p$  is changed from  $p=0$  to  $p=1.0$  by the step 0.1, and other parameters  $\langle n_0 \rangle$  and  $\gamma_L$  are determined by the minimum chi-squared method. The best fit is given by

$$p=0.8, \quad \langle n_0 \rangle=2.584, \quad \gamma_L=1.394,$$

with  $\chi^2_{\min}/\text{NDF}=372.4/32$ . As can be seen from Eq. (29), if we keep the relations that  $\alpha/\gamma_L=\text{const}$  and  $\beta/\gamma_T=\text{const}$ , we get the same minimum chi-squared value. The calculated multiplicity distribution is compared with the data in Fig. 2.

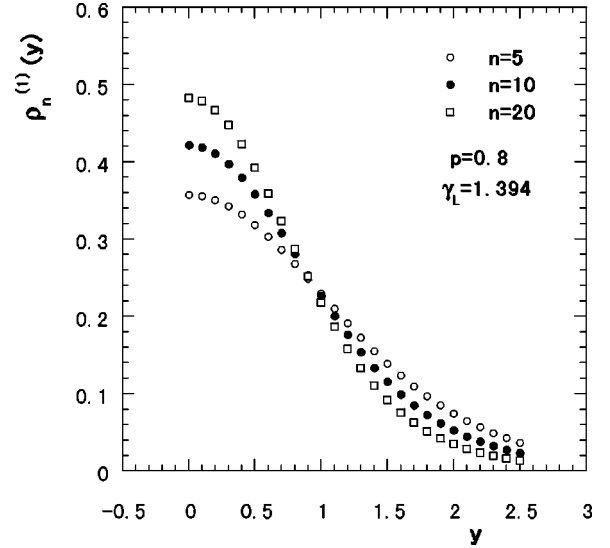


FIG. 3. Normalized one-particle rapidity distributions at fixed multiplicity calculated with  $p=0.8$ ,  $\langle n_0 \rangle=2.584$ , and  $\gamma_L=1.394$ .

For the sake of comparison, we also fit the data by the negative binomial distribution, which results in  $\chi^2_{\min}/\text{NDF}=465.0/33$ .

The normalized one-particle rapidity distribution at  $n$ -particle events is defined by

$$\tilde{\rho}_n^{(1)}(y)=\int \tilde{\rho}_n^{(1)}(y, \mathbf{p}_T) d^2 \mathbf{p}_T, \quad (33)$$

and calculated results for  $n=5, 10$ , and  $20$  are shown in Fig. 3. The peak height increases and the width of the distribution becomes narrower, as the multiplicity  $n$  increases.

In Fig. 4, the normalized two-particle rapidity distributions given by

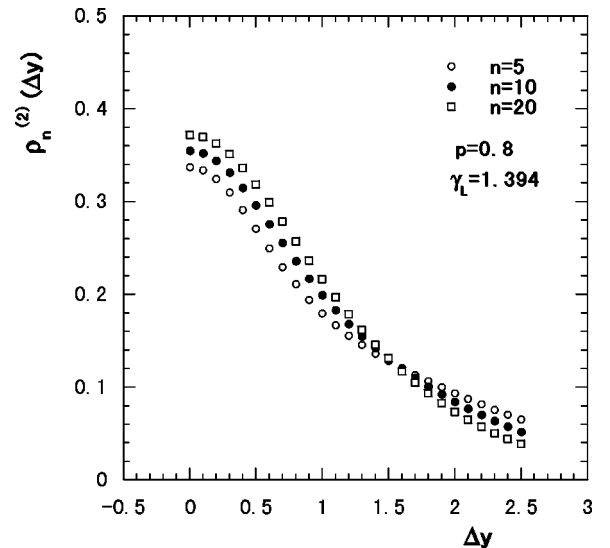


FIG. 4. Normalized two-particle rapidity distributions at fixed multiplicity calculated with  $p=0.8$ ,  $\langle n_0 \rangle=2.584$ , and  $\gamma_L=1.394$ .

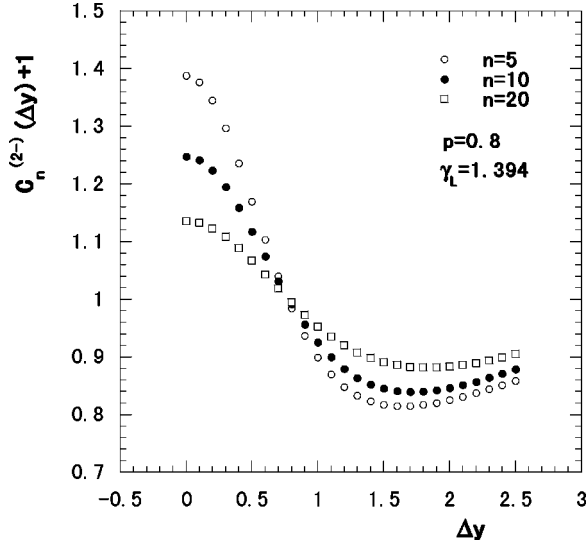


FIG. 5. Normalized two-particle correlation functions at fixed multiplicity calculated with  $p=0.8$  and  $\gamma_L=1.394$ .

$$\tilde{\rho}_n^{(2)}(\Delta y) = \int \int \int \tilde{\rho}_n^{(2)}(y_1, \mathbf{p}_{1T}, y_1 + \Delta y, \mathbf{p}_{2T}) dy_1 d^2 \mathbf{p}_{1T} d^2 \mathbf{p}_{2T} \quad (34)$$

are shown at  $n=5, 10$ , and  $20$ . The peak of the distribution

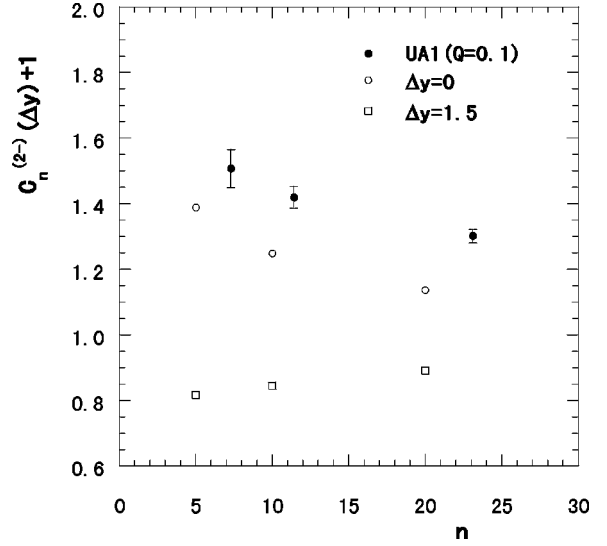


FIG. 6. Multiplicity dependence of normalized two-particle correlations. Solid circles show the data at  $Q=0.1$  GeV in  $p\bar{p}$  collisions [8]. Open circles and open squares are calculated with  $p=0.8$  and  $\gamma_L=1.394$ .

also becomes higher and its width becomes narrower, as the multiplicity  $n$  increases. However, the increasing rate is gentler than that of the one-particle density.

The normalized two-particle correlation function  $C_n^{(2-)}(\Delta y)$  at  $n$ -particle events is defined as

$$C_n^{(2-)}(\Delta y) = \frac{\int \int \int \tilde{\rho}_n^{(2)}(y_1, \mathbf{p}_{1T}, y_1 + \Delta y, \mathbf{p}_{2T}) dy_1 d^2 \mathbf{p}_{1T} d^2 \mathbf{p}_{2T}}{\int \int \int \tilde{\rho}_n^{(1)}(y_1, \mathbf{p}_{1T}) \tilde{\rho}_n^{(1)}(y_1 + \Delta y, \mathbf{p}_{2T}) dy_1 d^2 \mathbf{p}_{1T} d^2 \mathbf{p}_{2T}} - 1. \quad (35)$$

The calculated results on  $C_n^{(2-)}(\Delta y)$  at  $n=5, 10$ , and  $20$  are shown in Fig. 5. The multiplicity dependences of  $C_n^{(2-)}(\Delta y)$  at  $\Delta y=0$  and  $1.5$  are shown in Fig. 6, where the preliminary experimental data reported by the UA1 Collaboration at  $Q=0.1$  GeV are also shown.<sup>1</sup>

In  $e^+e^-$  collisions, the OPAL Collaboration published data on the multiplicity distributions [14] and multiplicity dependence of two-particle Bose-Einstein correlations [9] at 91 GeV. However, using the parameters adjusted to the observed multiplicity distribution, which is close to a Poisson distribution, calculated results on  $C_n^{(2-)}(\Delta y=0)$  are almost constant and do not show the  $n$  dependence. Next, the multiplicity dependence of the Bose-Einstein correlations at  $Q$

$=0$  GeV, which is estimated from the data with  $Q \geq 0.05$  GeV, is directly analyzed by our formula. We can fairly well reproduce the  $n$  dependence of the data with  $n_{\max}=27$ ,  $\alpha=0.125$ ,  $p=0.55$ , and  $\gamma_L=10.0$  if the minimum values of our calculated results on  $C_n^{(2-)}(0)+1$  are renormalized to 1. The result is shown in Fig. 7.

## V. SUMMARY AND DISCUSSION

Analytical formulas of the multiplicity distribution and particle densities in semi-inclusive events are derived from the generating functional GF in the presence of the chaotic and coherent fields. The formulas are applied to the analysis of the multiplicity dependence of two-particle correlations among identical particles in  $p\bar{p}$  collisions by the UA1 Collaboration [8] and in  $e^+e^-$  collisions by the OPAL Collaboration [9]. In the formula of the two-particle correlation, the multiplicity distribution and one-particle densities in semi-inclusive events are contained. Therefore, to fix the param-

<sup>1</sup>The data on the two-particle correlation are given by the variable four-momentum transfer squared,  $Q = \sqrt{-(p_1 - p_2)^2}$  GeV.  $Q=0$  corresponds to  $\Delta y=0$ . Therefore we compare our calculated results at  $\Delta y=0$  with the data at the smallest  $Q$  value ( $Q=0.1$ ) reported by the UA1 Collaboration.

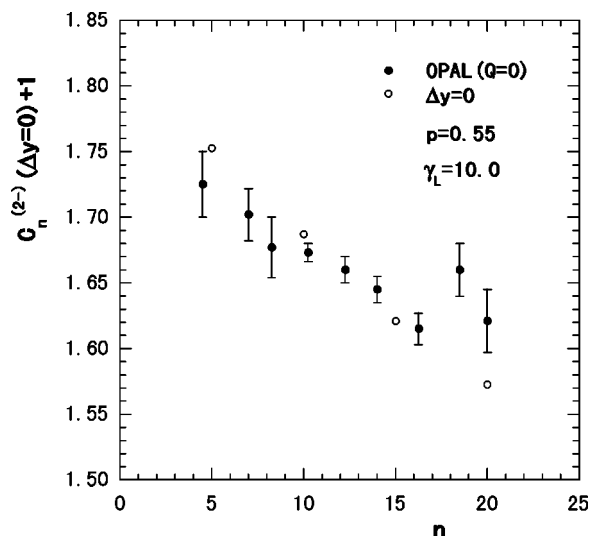


FIG. 7. Multiplicity dependence of normalized two-particle correlations. Solid circles indicate the values at  $Q=0$  GeV, estimated from the data with  $Q \geq 0.05$  GeV in  $e^+e^-$  collisions [9]. Open circles are obtained from our calculation at  $\Delta y=0$ .

eters in our formulas, at least the observed multiplicity distribution is necessary.

In  $p\bar{p}$  collisions, we adjusted the parameters using the multiplicity distribution taken from a different data sample from those of the two-particle correlation. Our calculated results with the constant chaoticity parameter reproduce well the gross features of the multiplicity dependence of the data, in spite of the values of  $C_n^{(2)}(0)$  being smaller than the data at  $Q=0.1$  GeV by about 20%. Some part of the deviation will be attributed to the fact that the parameters are determined by fitting the multiplicity distribution within a different pseudorapidity interval.

In  $e^+e^-$  collisions, we analyze the data of the two-particle correlation without fitting the multiplicity distribution. We can explain the multiplicity dependence of the two-

particle correlation at  $Q=Q_{\min}$  GeV observed in the experiment using the constant chaoticity parameter.

Calculated results on the normalized two-particle correlation in semi-inclusive events show that the peak of the distribution becomes lower as the multiplicity increases, even if the chaoticity parameter  $p$  is constant. This behavior is similar to the data of two-particle correlations in  $p\bar{p}$  collisions by the UA1 Collaboration and in  $e^+e^-$  collisions by the OPAL Collaboration.

In this paper, we analyze the data with the same values of chaoticity parameter  $p$  and correlation length  $\gamma_L$  in rapidity space. Our present analyses indicate that the coherent component is not negligible; in other words, the values of chaoticity parameters are smaller than 1. One possible candidate for the coherent component is a contribution from the decay products of long-lived resonances [15]. Another possibility to reduce the value of chaoticity parameter is contamination [16,3]. For example, about 20% of like-sign particles are not pions in the OPAL Collaboration data [9].

When the colliding energy of incident particles increases as in the forthcoming RHIC experiment, thousands of identical particles can be produced in an event. Then, the production domain of those particles can be analyzed precisely event by event. In general, the values of parameters will change according to the multiplicity. If the fitted values of chaoticity parameter or correlation length change suddenly at some multiplicity, it will be a possible signature that the threshold of a new phenomenon will open at that multiplicity.

#### ACKNOWLEDGMENTS

M.B. was partially supported by a Japanese Grant-in-Aid for Scientific Research from the Ministry of Education, Science and Culture (No. 09440103) and (No. 08304024). N.S. thanks A. Bartl, B. Buschbeck, and H. Eggers for valuable discussions. N.S. also thanks Matsusho Gakuen Junior College for financial support.

- [1] R. J. Glauber, Phys. Rev. **131**, 2766 (1963); in Proceedings of the Les Houches Summer School of Theoretical Physics, Grenoble, *Quantum Optics and Electronics*, 1964, edited by C. De Witt, A. Blandin, and C. Cohen-Tannoudji (Plenum, New York, 1965), p. 63; G. Lachs, Phys. Rev. **138**, B1012 (1965).
- [2] M. Biyajima, A. Bartl, T. Mizoguchi, N. Suzuki, and O. Terazawa, Prog. Theor. Phys. **84**, 931 (1990); **88**, 157 (1992).
- [3] N. Suzuki, M. Biyajima, and I. V. Andreev, Phys. Rev. C **56**, 2736 (1997); N. Suzuki and M. Biyajima, Prog. Theor. Phys. **88**, 609 (1992).
- [4] W. A. Zajc, Phys. Rev. D **35**, 3396 (1987).
- [5] S. Pratt, Phys. Lett. B **301**, 159 (1993).
- [6] W. Q. Chao, C. S. Gao, and Q. H. Zhang, J. Phys. G **21**, 847 (1995); Q. H. Zhang, Phys. Lett. B **406**, 365 (1997).
- [7] N. Suzuki and M. Biyajima, in *Proceedings of the 8th Inter-*

*national Symposium on Multiparticle Production "Correlation and Fluctuations '98,"* Matrahaza, Hungary, 1998, edited by T. Csörgő, S. Hegyi, R. C. Hwa, and G. Jancsó (World Scientific, Singapore, 1999), p. 98.

- [8] B. Buschbeck (private communication); B. Buschbeck, H. Eggers, and P. Lipa, in *Proceedings of the 8th International Symposium on Multiparticle Production "Correlation and Fluctuations '98"* [7], p. 28.
- [9] OPAL Collaboration, G. Alexander *et al.*, Z. Phys. C **72**, 389 (1996).
- [10] M. Biyajima, O. Miyamura, and T. Nakai, in *Proceedings of the Multiparticle Dynamics*, Hakone, Japan, 1978, edited by T. Hirose *et al.* (PIFP, Kyoto University, Kyoto, 1978), p. 139.
- [11] Z. Koba, H. B. Nielsen, and P. Olesen, Nucl. Phys. **B43**, 125 (1972); Acta Phys. Pol. B **4**, 95 (1973); L. S. Brown, Phys. Rev. D **5**, 748 (1972).



- [12] UA1 Collaboration, C. Albajar *et al.*, Nucl. Phys. **B335**, 1261 (1990).
- [13] P. Carruthers and Minh Duong-van, Phys. Rev. D **8**, 859 (1973).
- [14] OPAL Collaboration, P. D. Acton *et al.*, Z. Phys. C **52**, 539 (1992).
- [15] M. G. Bowl, Part. World **2**, 1 (1991).
- [16] J. G. Cramer and K. Kadija, Phys. Rev. C **53**, 908 (1996).